Materials Science & Engineering A 627 (2015) 182–190

Contents lists available at ScienceDirect

Materials Science & Engineering A

journal homepage: www.elsevier.com/locate/msea

The influence of ultra-fast annealing prior to quenching and partitioning on the microstructure and mechanical properties

Dorien De Knijf [a,*], Athina Puype [a], Cecilia Föjer [c], Roumen Petrov [a,b]

[a] Department of Materials Science and Engineering, Ghent University, Technologiepark 903, B-9052 Zwijnaarde, Ghent, Belgium
[b] Department Material Science and Engineering, TUDelft, Mekelweg 2, NL-2628 CD Delft, The Netherlands
[c] ArcelorMittal Global R&D Gent, Pres. J. F. Kennedylaan 3, B-9060 Zelzate, Belgium

ARTICLE INFO

Article history:
Received 28 October 2014
Received in revised form
24 December 2014
Accepted 30 December 2014
Available online 7 January 2015

Keywords:
Quenching and partitioning
Ultrafast annealing
Grain refinement
Microstructure
Mechanical characterization

ABSTRACT

The microstructural evolution of a Quenching and Partitioning (Q&P) steel after ultra-fast annealing (UFA) was studied and correlated with the obtained mechanical properties. The shift of the transformation temperatures with increasing heating rates was shown by dilatometric experiments. The influence of the heating rate on the carbide precipitation and texture was evaluated. A remarkable refinement of the prior austenite grain size is observed resulting in a better combination of strength, ductility and fracture behavior compared to conventionally used heating rates.

1. Introduction

The classical development of advanced high strength steels (AHSS) is usually based on special combinations of alloying elements or on controlling the cooling rate. Nowadays non-conventional, novel process techniques have been developed to refine the microstructure and to improve both strength and toughness. Recent publications [1,2] suggested that rapid transformation annealing cycles applied to cold rolled AHSS, can result in substantial grain refinement. The degree of refinement is influenced by the interaction between recrystallization and ferrite-to-austenite phase transformation [1]. Recrystallization in cold rolled AHSS is delayed to higher temperatures with increasing heating rate and possibly even to temperatures above A_{c1}. Hence α–γ phase transformation starts in a non-recrystallized matrix with a large number of nuclei which results in remarkable grain refinement [1,3]. Carbon and alloying elements play an important role in controlling the grain size in conditions of fast and ultrafast heating. The effect of grain refinement is clearly pronounced in C–Mn steels whereas for interstitial-free and low carbon steel, the grain structure and recrystallization texture were not significantly altered by applying higher heating rates or shorter soaking times [4–7].

It was reported that at heating rates as high as 3000 °C/s, the phase transformation is primarily located in the subgrain boundaries of the recovered matrix [8,9]. During recovery, the dislocations in the cold deformed matrix are re-arranged in subgrain boundaries forming cells (polygons) with dislocation walls. These dislocation cells play an important role as carbon diffusion channels in the transformation process. Faster carbon diffusion in the cell walls leads to local increase of the C-concentration and formation of fine carbides which pin the dislocations, suppress their movement and therefore inhibit growth of the recrystallized grains. Hence according to [8,9], a very important parameter for grain refinement during ultra-fast annealing is the distribution and size of the iron carbides in ferrite. A homogeneous distribution of small carbides impedes the coarsening of recrystallized ferrite grains as well as a homogeneous nucleation and growth of very small austenite grains. If the carbides are coarse or in the "carbide free" zones of not uniformly distributed carbides, the growth of the recrystallized ferrite grains during annealing is not inhibited. Moreover, non-uniformly distributed zones of fine austenite grains can develop where the initial carbides were present.

The aim of the present work is to bring insight into the possibilities of refining the microstructure of Q&P steels prior to the partitioning stage of the Q&P heat treatment and the corresponding influence on the final mechanical properties.

2. Experimental

Hot and cold rolled steel with a nominal composition of 0.25C–1.5Si–3Mn (wt%) was studied in this work.

* Corresponding author. Tel.: +32 9 331 04 41; fax: + 32 9 264 58 33.
E-mail addresses: doriendeknijf@hotmail.com, dorien.deknijf@ugent.b (D. De Knijf).

http://dx.doi.org/10.1016/j.msea.2014.12.118
0921-5093/

2.1. Heat treatments

To determine the variation of the transformation temperatures as a function of heating rate, experiments were carried out in a Bähr DIL 805A/D dilatometer on hot rolled rectangular samples with dimensions of $2.5 \times 3.5 \times 10\ mm^3$, with the longest axis parallel to the plate rolling direction. The samples were heated with different heating rates of 10 °C/s, 150 °C/s, 500 °C/s, and 1000 °C/s up to 1000 °C which is in the austenitic region and cooled at 20 °C/s to room temperature.

Strips of 80% cold-rolled sheets ($100 \times 10 \times 0.5\ mm^3$) were cut parallel to the rolling direction and subsequently subjected to ultra-fast heating Q&P cycles in the Gleeble™ thermo-mechanical simulator (cfr. Fig. 1). The cold rolled strips were reheated to 850 °C without isothermal holding at three different heating rates of 10 °C/s, 500 °C/s and 1000 °C/s. An additional heat treatment was performed with a heating rate of 10 °C/s to 850 °C at which the sample was kept isothermally for 5 min to simulate a conventional Q&P cycle. Subsequently, the samples were cooled at 20 °C/s to 270 ± 10 °C. The used quench rate of 20 °C/s was higher than the critical cooling rate to avoid ferrite, pearlite or bainite formation during cooling, which for this steel composition was determined to be 10 °C/s. Afterwards the samples were reheated at 10 °C/s to 400 °C for 50 s to complete the partitioning step and finally cooled with N_2-gas to room temperature.

2.2. Microstructural characterization

For microstructural characterization, the samples were mechanically ground and polished following the classical preparation route.

SEM images and EBSD maps were obtained by a FEI Quanta™ 450-FEG-SEM equipped with a Hikari EBSD detector controlled by the EDAX-TSL OIM-Data Collection software. The EBSD data were acquired on a hexagonal scan grid using an accelerating voltage of 20 kV, a working distance of 16 mm, tilt angle of 70° and a step size of 60 nm. The orientation data were post-processed with TSL-OIM Analysis 6.2® software and only the points with a confidence index higher than 0.1 were considered in the scan. Average grain sizes were determined on the base of a grain definition of minimum 4 pixels per grain and a misorientation angle of 15°.

The austenite volume fractions were determined at room temperature with XRD experiments performed on a Siemens Kristalloflex D5000 diffractometer equipped with Mo-K_α source operating at 40 kV and 40 mA. A 2θ-range of 25–45° was scanned using a step size of 0.01°, dwell-time of 2 s and rotation speed of 15 rpm. The data were post-processed by subtracting the background radiation and $K\alpha_2$ influence. The retained austenite volume fractions were determined with the formula of Cullity [10] using the intensity of the $(220)_\alpha$, $(311)_\alpha$, $(200)_\gamma$ and $(211)_\gamma$ reflections.

2.3. Mechanical testing

Tensile tests were performed at room temperature on A25 tensile test samples (ASTM E8/E8M) on a MTS819 tensile test machine at two strain rates −0.083 mm/s until an elongation of 2.5 mm followed by a strain rate of 0.208 mm/s until fracture.

3. Results

3.1. Dilatometer experiments on hot rolled material

3.1.1. Shift of the transformation temperatures

Samples of the hot rolled steel were heated in the dilatometer up to a full-austenisation temperature of 1000 °C, with heating rates of 10 °C/s, 150 °C/s, 500 °C/s and 1000 °C/s. Analysis of the dilatation records illustrates that both the A_{C1} and A_{C3} temperatures increased with higher heating rates, cfr. Fig. 2. The A_{C1} and A_{C3} temperatures increased from 736 °C to 783 °C and 793 °C to 873 °C, respectively upon changing the heating rate from 10 °C/s to 1000 °C/s. The ferrite fractions at 850 °C (which was the reheating temperature for the cold rolled samples) were calculated by the lever rule as shown in Fig. 2. After reheating the sample with 500 °C/s to 850 °C, the steel is almost completely austenitized, however, after reheating at 1000 °C/s and subsequent quenching about 25% ferrite remains in the material. The reheating experiments confirm the well-known fact that the A_{C3} is more sensitive to the heating rate then the A_{C1} temperature (as can be seen from the slope change of the curves in Fig. 2).

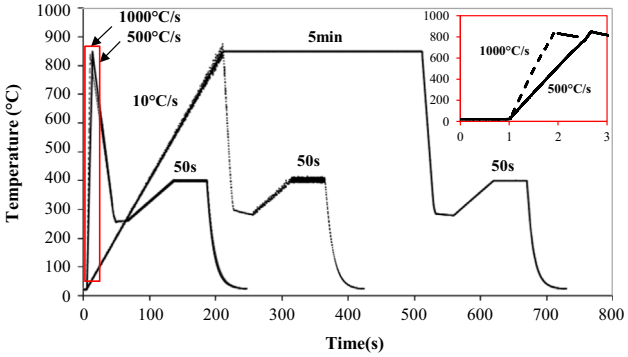

Fig. 1. Heat treatment cycles performed in Gleeble on the cold rolled material, upper right corner insert is a zoom of the first 3 s of the heating time.

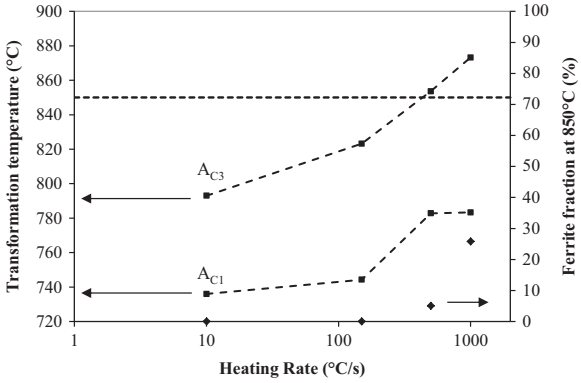

Fig. 2. Shift of the transformation temperatures A_{c1} and A_{c3} with heating rate together with the theoretical calculated ferrite fraction upon heating to 850 °C.

3.1.2. Carbide precipitation conditions

In Fig. 3(a–e), the carbide precipitation conditions were studied by scanning electron microscopy in the hot rolled sample and the quenched samples which were heated at different rates. The pearlitic microstructure of the hot rolled material is given in Fig. 3(a). After conventional flash heating with 10 °C/s and quenching, a very small fraction of carbides is detected in the microstructure, cfr. Fig. 3(b). An increase of the heating rate to 150 °C/s leads to an increasing fraction of undissolved carbides which are present in the microstructure as (partially) spheroidized pearlitic cementite, cfr. Fig. 3(c). At a heating rate of 500 °C/s, a smaller part of the carbides is dissolved as can be observed in Fig. 3(d). The shape of the original cementite in the pearlite is more distinctly visible which implies that the carbides are partially spheroidized cementite. After reheating with 1000 °C/s, the remaining carbides are finer and with well pronounced lath-shape (cfr. Fig. 3(e)) with similar morphology to the cementite lamellas in pearlite (cfr. Fig. 3(a)) which is an indication that they are undissolved pearlitic cementite.